

A Photogrammetric System for Model Attitude Measurement in Hypersonic Wind Tunnels

Thomas W. Jones* and Charles B. Lunsford†
NASA Langley Research Center
Hampton, VA 23681

A series of wind tunnel tests have been conducted to evaluate a multi-camera videogrammetric system designed to measure model attitude in hypersonic facilities. The technique utilizes processed video data and photogrammetric principles for point tracking to compute model position including pitch, roll and yaw. A discussion of the constraints encountered during the design, and a review of the measurement results obtained from the NASA Langley Research Center (LaRC) 31-Inch Mach 10 tunnel are presented.

I. Introduction

THE LaRC 31-Inch Mach 10 tunnel has a closed 31 x 31 inch test section with a contoured three-dimensional water-cooled nozzle to provide a Mach number capability of 10.¹ A hydraulically operated, side-mounted model injection system injects the model into the flow after the flow stream has been preheated. The hydraulic injection/retraction support mechanism is capable of providing an angle-of-attack (AoA) range of $\pm 90^\circ$. The sideslip (Yaw) range of motion is $\pm 5^\circ$. The model support mechanism also includes the mechanical position feedback sensors that provide pitch and yaw measurements. These sensors have good accuracy but fail to account for deflections to model attitude caused by sting bending from aerodynamic loads. The resulting implications are a potential for lower quality information on the test article pitch, yaw and roll states. In many cases, large uncertainties enter the angular measurement process, which in turn, requires repeated testing and data averaging techniques to accomplish test objectives. A view of the facility and the model injection system is provided in Figure 1.

As is the case for most hypersonic wind tunnel facilities, the class of models tested typically excludes on-board instrumentation. While servo accelerometers are routinely used for angle-of-attack measurements in most large-scale wind tunnel facilities,² their size and additional packaging requirements have prevented their use in this class of model. Sting loading conditions that effect model attitude can be estimated, but the need for an independent off-body measurement system to accurately measure this deflection and provide a more accurate indication of the model's true position is the driving force behind this design and development effort.

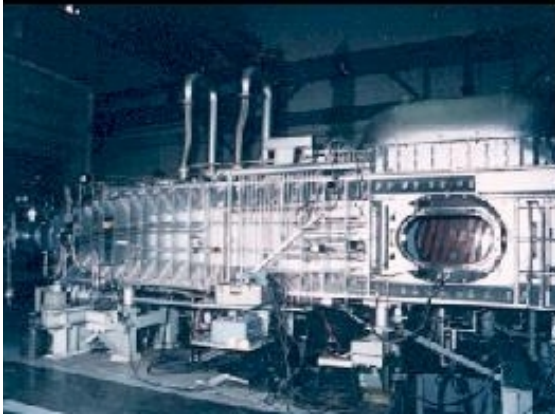
II. Aerodynamic Testing Requirements

While there are many advanced hypersonic concept configurations that only test over very small angle of attack ranges near zero, there are various configurations that do require testing at a high angle of attack. At these conditions the associated flow physics is complex and may exhibit attached oblique shocks, detached bow shocks, large regions of separated chaotic flow, body generated vortices, and thick turbulent boundary layers any of which may greatly influence model dynamics and the associated sting bending.³

These characteristics will be highly dependent on aerodynamic angle of attack, thus requiring a high fidelity model orientation measurement capability over a large range of the test section's operational area. The current industry-government program goals are to achieve an angular wind tunnel measurement resolution of 0.1 deg or better.⁴

* Aerospace Engineer, Advanced Sensing and Optical Measurements Branch, M/S 238, non-Member AIAA.

† Aerospace Engineer, Advanced Sensing and Optical Measurements Branch, M/S 238, non-Member AIAA.



(a. 31-Inch Mach 10 Air Tunnel



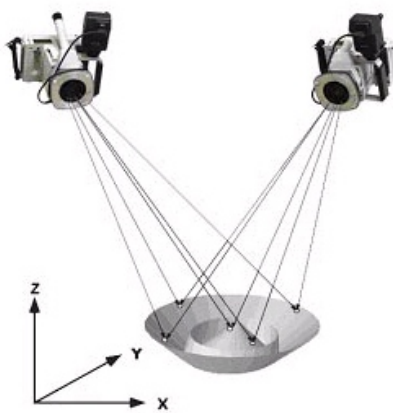
(b. Model injection system – 31-Inch Mach 10 Tunnel

Figure 1. NASA Langley Hypersonic Facilities

III. System Design

A recent modification to the facility now provides optical access to the test section from three of the four sides. This modification enables video based measurement systems to be considered as a leading candidate for obtaining model attitude data. To meet the aerodynamic test requirements, a two-camera video system was designed that employed the basic principles of photogrammetry.

Photogrammetry is the science of measuring the location and size of three-dimensional (3D) objects with photographs. The data analysis procedures are related to those used in surveying. When dealing with time sequences of images, this technology is often called “videogrammetry” (or “videometrics”) instead of “photogrammetry”. High-contrast circular retroreflective targets are usually installed on the object to serve as discrete points when the highest measurement accuracies are required. These measured sets of object points can characterize static shape or position. The images of the targeted points are processed to determine the 3D coordinates of the discrete points on the object’s surface by triangulating the correspondence of intersecting light rays for the point. A diagram of the technique is depicted in Figure 2, for the purpose of demonstration there are 2 cameras shown. Even though processing requirements for a photogrammetric solution can be intensive, the capacity of modern PC workstations makes photogrammetric results possible in real time.



Multiple point triangulation

Figure 2. Photogrammetric triangulation of intersecting light rays for 3D point determination.⁵

For this application the camera specifications were partially derived from the maximum desirable target size. An assumption was made that the small surface area of the models usually tested in hypersonic facilities would restrict the size of surface targets to no larger than 2 mm. The retroreflective targeting material has a surface thickness of 0.004 inches, and to help minimize the flow disturbance, an acrylic coating is applied to feather the edges of the target. To support high accuracy sub-pixel centroid determination, a minimum diameter of 5 pixels on the image plane is needed from each of the targets. To accurately track the model through its range of motion a minimum of 5 targets are desired. The target size and the estimated working distance from the model dictated the need for a 1 mega-pixel class camera.

The cameras selected were high-resolution Hitachi KP-F120’s, they utilize a 2/3 inch CCD sensor with a 1392 x 1040 resolution. This camera provides optimum centroid determination for 2 mm targets when viewed through a 12.5 mm lens at a distance of approximately 1 meter.

The cameras are synchronized and provide data output rates (i.e. frame rates) as high as 30 hertz (Hz.). A diagram of the camera arrangement using the tunnel's top optical access window is provided in Figure 3.

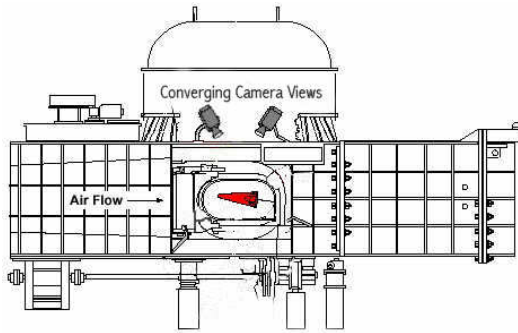
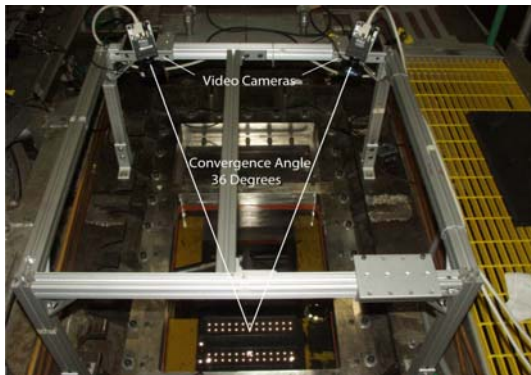


Figure 3. Camera-tunnel arrangement

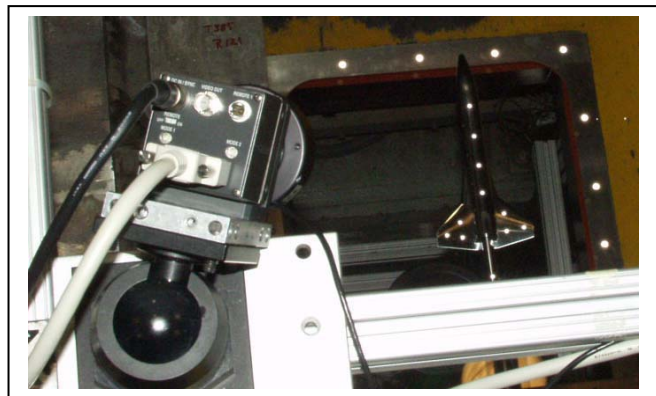
to achieve the highest accuracy, the two-camera system should maintain a 60-90 degree convergence angle. However, the size of the access window on top of the test section restricted the camera separation to approximately 36 degrees. The measurement accuracy in the pitch axis could be increased by locating the system at the side window port, but this would complicate tunnel access since the side window/door port provides the primary test section access.

Testing at the 31 inch facility identified the best optical access point to achieve the maximum measurable pitch range using the fixed position two-camera setup. The orientation selected is forward facing with converging views to record the model position. In the configuration shown in Figure 4a, the system is capable of tracking a model with surfaces parallel to the flow over a range of -20 to 40 degrees. The technique derives model position from an array of retroreflective targets on the model that are tracked throughout a recorded video sequence.

Figure 4b shows the view of a typical hypersonic model with attached retroreflective targets in the 31 inch tunnel test section with the video camera in the foreground.



(a. Video camera convergent view configuration



(b. Representative view of model in test section

Figure 4. Camera mechanical support hardware

The system is built on a T-slotted aluminum frame (Figure 5.) that allows the cameras to be quickly and easily repositioned. The system is also portable; the aluminum frame supports a side mounted power/data distribution panel that regulates all of the power, control and data for the cameras and lighting, making the system completely self contained. To support the need for long cable lengths, fiber optic converters were added to convert and transmit the digital data from the cameras.

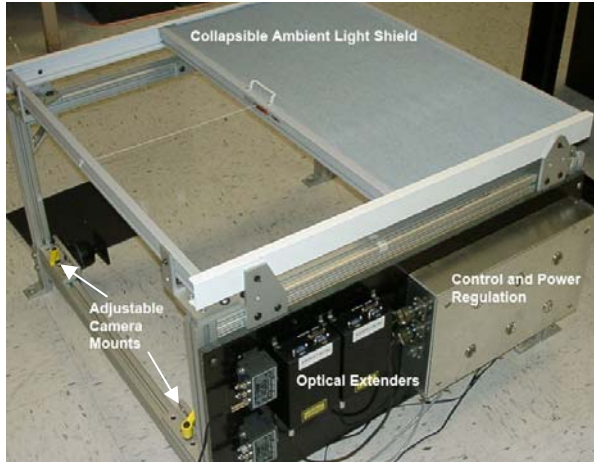


Figure 5. Test section camera mounting structure

A. Processing Algorithm

Photogrammetry offers several derivation methods for resolving camera parameters and object space coordinates. For our application a four-step approach is followed. The first step is the pre-run calibration to determine the camera parameters, specifically the principle distance (focal length), lens distortions, and perspective center. The second step, a statistically less rigorous technique known as “Resection” will be used to determine the camera’s position and orientation. Resection relies on an existing knowledge of the coordinates of multiple control points. For this case the coordinates of the control points, located on the floor of the test section, have been independently established to a high level of accuracy to minimize the potential bias error that may be introduced throughout the calculations.

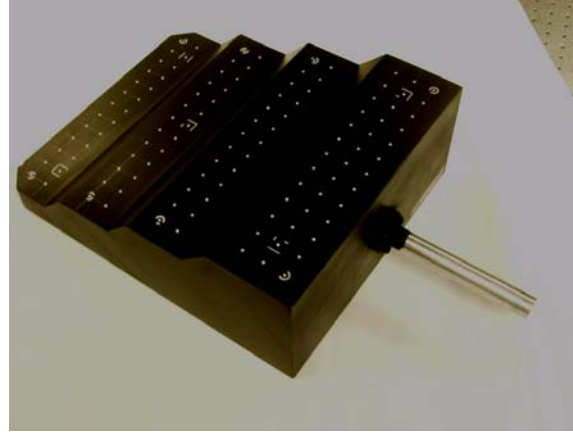
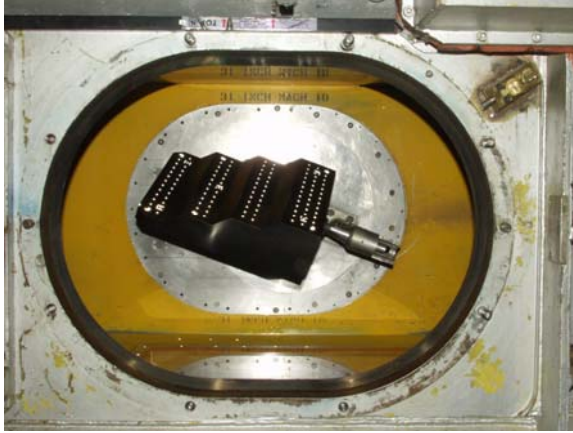
The camera orientation angle and location of the perspective center are referred to as the exterior orientation parameters. For a camera, the relationship between object space point, perspective center and image point is described by the collinearity equations,⁶ the fundamental equations of photogrammetry.

The third step in determining the object space coordinates of the targets is known as “Intersection”, for this step it is assumed that the exterior orientation parameters have been successfully determined through resection. For the intersection process, the object space co-ordinates of a target on the model can be determined by a least squares estimation of the collinearity equations.

The final step derives the model’s angular position by treating all targets on the model as a rigid body. The computed global coordinates of the targets are inputs to the solution. The model’s position is based on a three dimensional similarity transformation between the zero position, obtained as a wind-off zero point, and the measurements computed throughout the tracking process. A least squares estimation solution is used to reconcile redundant target coordinate data and appropriately process the statistical fluctuations of the measured target locations.⁷ The calculations include a full error propagation of the precisions of the tracked target coordinates into the solution and therefore provide precisions or uncertainty limits for pitch, roll and yaw. While the data presented here was post processed to insure accuracy, the algorithm is under development to support real time operations.

B. Calibration

The general technique for camera calibration in a photogrammetric measurement system requires the recording of a series of images of a known target field from multiple perspectives. The images are then used to perform a camera calibration, determining the principal point location, principal distance, and lens distortions. In addition, the process establishes a coordinate system through the determination of the camera’s relative orientation from which all measurements are based. However, in this case, access to the tunnel test section area is limited due to safety issues both before and during any test. Therefore it was required to develop a calibration technique that didn’t require removing the cameras and delaying tunnel operations each time a calibration is required. To meet this requirement a sting-mounted calibration plate was designed to provide the ability to perform in-situ calibrations, Figure 6a. shows the plate in the test section of the 31-inch hypersonic facility. The calibration plate is injected into the tunnel in a wind-off condition and the host computer then records images of the calibration plate at various pitch angles. The calibration plate is attached to the model support system in the same manner as a model, its embedded sting, visible in Figure 6b. provides the means to support easy installation and removal.



(a. Test section view sting-mounted calibration plate

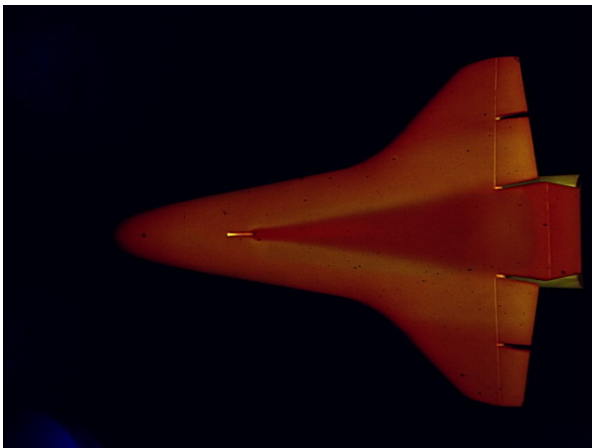
(b. Calibration plate with sting mounting adapter

Figure 6. Video camera calibration plate

C. Lighting

In most videogrammetric applications targets are illuminated with a general white light source. However, phosphor thermography a color imaging based measurement system is routinely used in the Langley hypersonic facilities.⁸ Therefore, the design of a parallel imaging technique needed to consider the lighting issues required for this technique. The phosphor technique utilizes a Ultra-violet (UV) source that is absorbed by the phosphor coating on the model and emits a response in the visible range based on the thermal profile of the model.

The videogrammetric system was designed to prevent interference with the phosphor’s source lighting (UV) and the measured response in the visible spectrum of the model during testing. To accomplish this, target illumination for the videogrammetric system was designed to operate in the near IR region (860 nm) to prevent interference from both ambient lighting and the phosphor thermography technique. A commercially available lens mounted LED light ring was specified for this requirement. To further enhance the contrast, optical filters were added to the lens to block all visible sources below 700 nm. To evaluate the efficiency of the lighting system design, a phosphor thermography test was conducted with both test techniques active during data recording. The cameras and lighting for the two techniques were positioned in opposite windows with the phosphor camera system viewing the model from the side window and the videogrammetry system viewing from the top test section window. A simultaneously recorded image of the model as viewed by each system is visible in Figure 7. There is no evidence of cross system interference from either systems perspective.

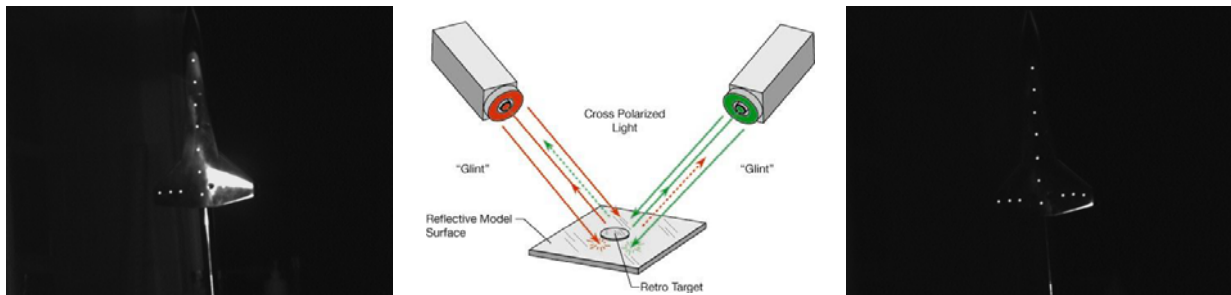


(a. UV illuminated model

(b. IR illuminated targets for AoA tracking

Figure 7. Concurrently recorded images during Phosphor Thermography model testing.

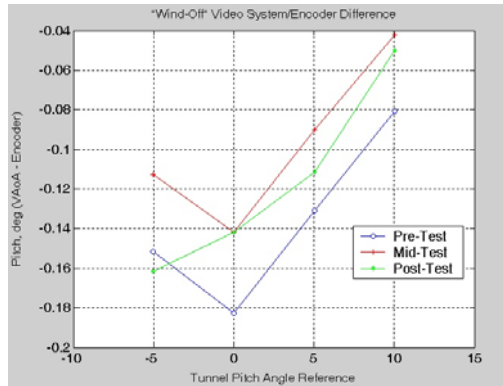
While phosphor model testing in the hypersonic facilities represents a significant percentage, polished surface stainless steel models represent a greater percentage of tests. Stainless steel models have traditionally presented problems to image based measurement systems due to the reflections and glints from the surface, causing target occlusions. An example of a model image with significant target occlusions is shown in Figure 8(a). In general when illuminated, retroreflective targets reflect the light back to the source along the incident axis. In the case where the targets are attached to a reflective surface such as a polished steel model, the model itself will act like a mirror and reflect a majority of the light. This effect can be detrimental when the light is reflected back to the imaging camera effectively “washing out” the target points.. To combat this effect a cross-polarization technique has been developed that greatly reduces the glints and reflections.⁹ The technique as illustrated in Figure 8(b) has a polarizing filter in front of the LED array and the camera. The polarizers are aligned such that the LED lighting produced by each is crossed relative to the other. The polarization angle of the camera filter is aligned to match that of the attached LED light. The polarization angle of the camera filter blocks the light from the second camera’s LED source that is polarized to an angle offset 90 degrees relative to the first camera’s. The result using this technique on models with relatively planar surfaces is positive, the model tested shows significant improvement in image contrast with this technique. Images from the same camera recorded with and without the polarization are shown in Figure 8(a) and (c). While the effectiveness of the technique is largely dependent on the model shape, most models tested in this class of facilities do not include complex geometries that may limit the effectiveness of the technique. Further studies of this technique are the subject of additional investigations.



(a. Image recorded without polarizer (b. Two camera cross polarization (c. Image recorded with x-polarizer
Figure 8. Cross polarization technique for glint removal

IV. Integration and Testing

The pitch encoder was calibrated with an independent angle measurement system (AMS). The AMS has a NIST traceable 2σ pitch accuracy after calibration of 0.002° between $\pm 30^\circ$. For calibration, the AMS was mounted to the model (Figure 9a), a wind-off polar was performed over a range of -5° to 10° in 5° increments. To identify any potential shifts in the encoder, this exercise was repeated three times during the course of the test. The output from the encoder and the AMS were monitored and individual regressions were performed on the sensor against the AMS reference. The wind off accuracy for the three separate readings from the tunnel encoder indicates the encoder has a bias error of greater than -0.1° over most of the measurement range (Figure 9b). Analysis of the calibration data indicates a bias error over the test range, but a more detailed evaluation using a randomized pattern of points that are approached from both the positive and negative side of the desired angle would be required to accurately map the overall bias error of the sensor. The data system applied a correction to the recorded data during the actual test reflecting the calibration.



a). Encoder calibration (wind-off) with AMS b). Pre & post test cal checks

Figure 9. Tunnel AoA system in-situ calibration

For this evaluation the targets on the floor (visible in Figure 4b.) of the test section provided a planar reference to check the computed angle of attack measurements generated by the video system. The encoder will provide a backup measure of comparison.

For the actual test a series of 10 tunnel runs were conducted over a four-day period to benchmark the performance and identify any critical problems and deficiencies. Future testing will aim to fully characterize the uncertainty by using an independent validation method. Data comparisons for each run were made based on the measurements derived from the 12 retro-reflective targets on the model. The targets were tracked throughout the range of motion and compared with those measurements simultaneously recorded from the model support system (M_{ss}) pitch angle encoder. The comparisons were based on computed wind tunnel measurements recorded during a pitch sweep over a range of -5 degrees to $+10$ degrees. Pitch pause sweeps were automatically performed under computer control. A 2 sec. dwell time was maintained at each pitch angle to allow for steady state evaluation.

Frequently the wind tunnel measurement is desired in a steady state condition; however model configuration and run conditions often create model dynamics that require the point measurements to be averaged. The model configuration for this test produced marginally detectable vibrations. It should be noted that the modestly low frame rate (30 Hz.) of the cameras might have limited the ability to measure higher frequency dynamics. The pitch sweep shown in Figure 10 is typical of those performed throughout this evaluation. The model was injected at a zero degree pitch angle and incremented by 1 degree steps from -5 degrees to $+10$ degrees pitch. Wind tunnel conditions were maintained at a stagnation pressure of 1450 psia and a stagnation temperature of 1250 R throughout the run sequence for each test.

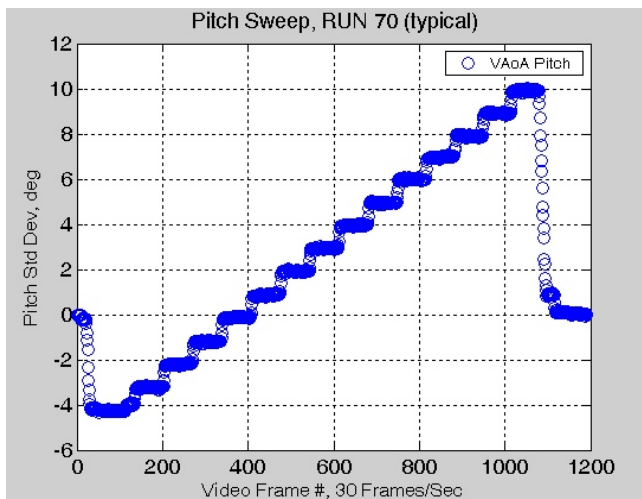


Figure 10. Pitch sweep performed for system evaluation

The plots shown in Figure 11 magnify the variance in the calculated pitch angle throughout the sweep. Two randomly selected runs are shown as examples. To better visualize and compare the scatter or noise, the referenced angle (i.e. -4,-3,-2,... 8,9,10) was subtracted for the respective points in each polar. The points were shifted where necessary to provide a zero base reference to aid in the evaluation.

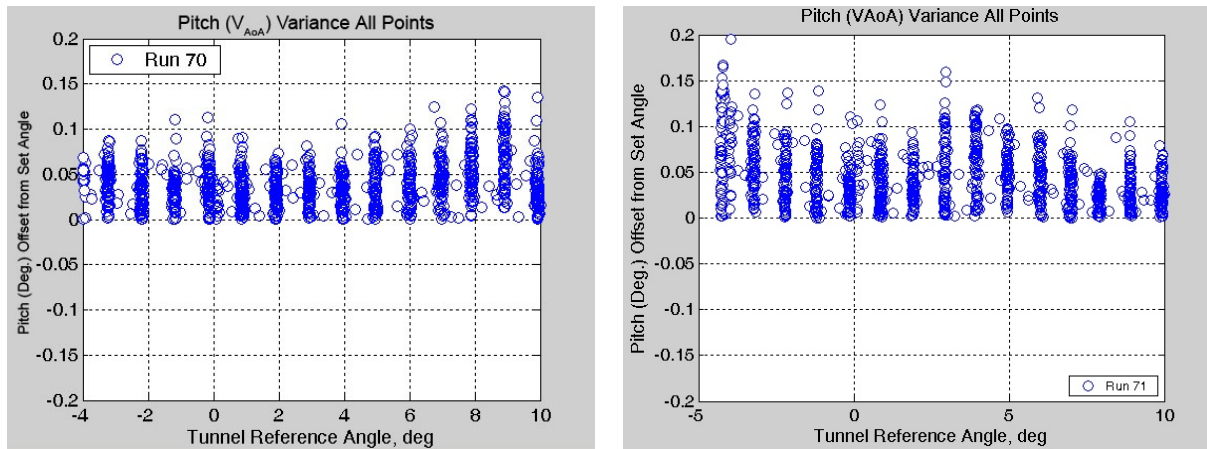


Figure 11. Pitch; noise level or scatter from two randomly selected runs

To evaluate the stability of the “on-point” measurement, four runs were analyzed at the randomly selected 5-degree position. The data was averaged over the 2s period for each run independently providing 60 raw points per averaged data point. The data in Figure 12 provides a closer look at the variance, at the 5 degree point in each of 4 pitch sweeps. Analysis identified a mean of 5.04 degrees with a 1-sigma of 0.0231, 0.0237, 0.0232, and 0.0231 for each run 68-72, respectively.

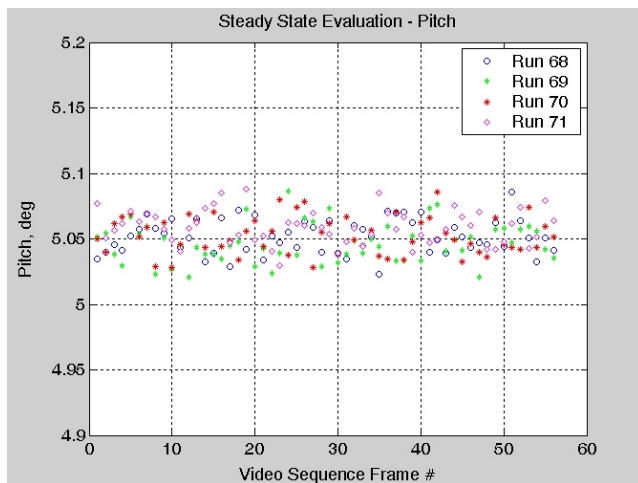


Figure 12. Steady state analysis of pitch at 5 degree pt.

for roll and yaw. The data shown in Figure 13 represents the calculated roll and yaw for two runs which was typical of that for all runs. To account for the possible differences in coordinate system alignment between the video system and the model positioning system, the values were calculated representing the difference in position relative to the wind-off measurement as derived by the video system. Analysis of the data indicates a notable change in roll as the model approaches higher angles of attack. The change is concluded to be attributable to sting bending. As expected the yaw encoder maintains a zero value throughout the test. Future testing will include independent methods for validating the full 3-axis position.

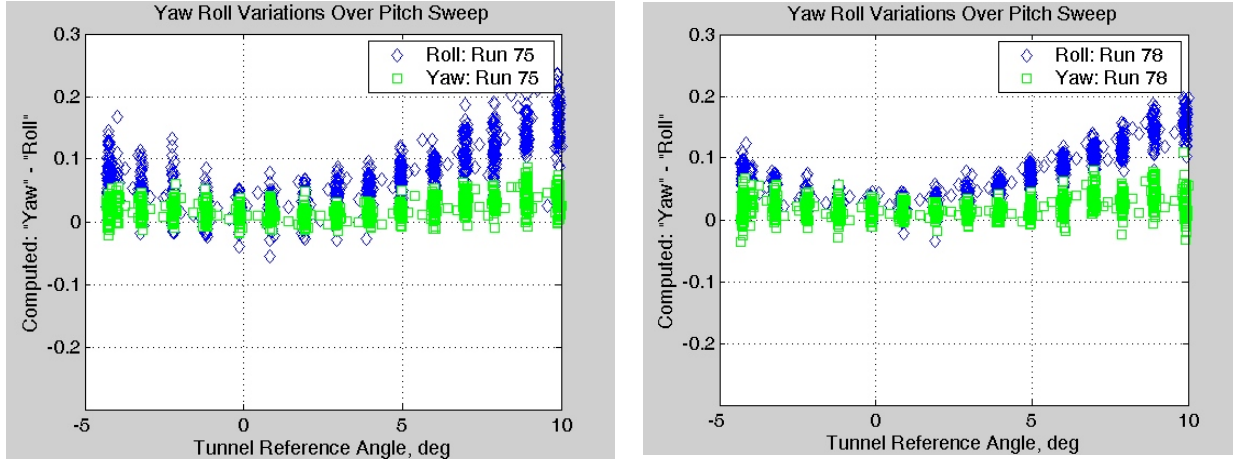


Figure 13. Measured Roll and Yaw over full range of pitch polar, evidence of sting bending at higher pitch.

To investigate the difference between the runs with the available data, we evaluated the rigid body transformation used to determine the 3D position on a point-by-point basis. A Unit Weight Estimate (UWE) was calculated for each point, the results are shown in Figure 14. The UWE is sigma-zero for the least squares estimation solution to the 3D transformation. It measures the "goodness of fit" and larger numbers (>1) indicate a poorer result. For this application data supports the idea that the points and thus the model are a rigid non-flexing structure. The analysis indicated a very good point-to-point transformation for each run. However, the scatter in the computation at the larger angles indicates a possible error in the coordinate transformation or the model alignment process. Both are aspects that require further investigation to adequately resolve the error.

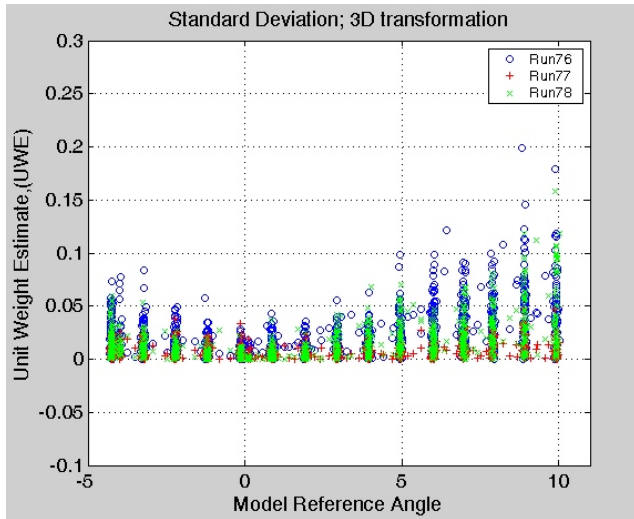


Figure 14. Least squares estimate for 3D transformation

in pitch over an angle of attack range of 15 degrees. To better understand the systems performance in the wind tunnel, a series of tests with an independent validation are needed. The tests will need to include a full characterization of the bias between the systems over the measurable range with and without air flow for pitch, roll and yaw.

Various constraints including lighting, optical access and calibration associated with the system design were investigated and described in this report. An innovative lighting technique using cross-polarization was demonstrated to substantially reduce glints and unwanted reflections for dual camera configurations. The technique's operation does not interfere with other techniques such as phosphor thermography and should be adaptable to other facilities.

Optical access to the tunnel test section was gained through a top view window. This perspective allows target tracking over a large angle of attack range. The choice of locating the system on top of the test section may yield the weakest results in the pitch axis, a by product of the small separation (convergence) angle between the two

V. Conclusions

The development of an angular measurement system for hypersonic wind tunnel facilities is considered in this effort. The use of 2 mega-pixel type video cameras and photogrammetric processing techniques in a prototype demonstration is addressed. All major aspects of the system design have been investigated. Camera calibration, lighting, data acquisition, target tracking, and model attitude derivations were explored and investigated to a level that confirmed acceptable performance. The operational capability was tested and demonstrated in wind tunnel run conditions.

The angular measurement performance based on the wind tunnel data was positive, but not independently validated. The measurement accuracy met the design requirement of 0.1 degree

cameras, but preliminary indications imply the effect on measurement accuracy is not significant. Improvements in the measurement accuracy in the pitch axis could be made by locating the system at the side window port, but this would restrict tunnel access.

To minimize impact on tunnel operations an in-situ calibration technique using a sting mounted 3D calibration plate was developed. The calibration plate will allow routine calibration of the cameras without requiring special test section access.

Although the actual system has not been fully integrated into the Langley 31-Inch facility, the functional performance of the system in the facility demonstrates the system's capabilities. The system design is non-contact and non-intrusive in terms of the model and support system, only requiring a few 2 mm retroreflective targets. System calibrations are typically required only once per test. The portable self-contained nature of the system allows the system to be easily adapted to other hypersonic wind tunnel facilities at NASA LaRC. The conclusion drawn from this design effort is the angular measurement of hypersonic class models using mega-pixel type video cameras and photogrammetric processing techniques is capable of satisfying current accuracy objectives.

1 J. R. Micol, Langley Aerothermodynamics Facilities Complex: Enhancements and Testing Capabilities , 36th AIAA Aerospace Sciences Meeting and Exhibit, Reno, Nevada, AIAA 98-0147, January 12-15, 1998, (4MB).

2 T. Finley and P. Tchong, "Model Attitude Measurements at NASA Langley Research Center", 30th Aerospace Sciences Meeting & Exhibit, January 1992, Reno, NV, AIAA 92-0763.

3 B. Newman and Si-bok Yu, "Development of a High Accuracy Angular Measurement System for Langley Research Center Hypersonic Wind Tunnel Facilities," NASA/CR-2003-212401, Langley Research Center Hampton, Virginia, August 2003.

4 Tripp, J.S., Tchong, P., Burner, A.W., and Finley, T.D., "Summary Report of the First International Symposium on Strain Gauge Balances and Workshop on AoA/Model Deformation Measurement Techniques," NASA-CP-1999-209101, Langley Research Center Hampton, Virginia, March, 1999.

⁵ Geodetic System Inc., www.geodetic.com, Melbourne FL USA

6 K.B. Atkinson, Close Range Photogrammetry and Machine Vision, Whittles Publishing, Scotland, UK, 1996, pp. 24-27.

7 W.L. Snow, M.R. Shortis, "A Rigid Body Motion Analysis System for Offline Processing of Time Coded Video Sequences", Videometrics IV, SPIE Proceedings Vol 2598, Oct 1995.

8 N. Ronald Merski, Reduction and Analysis of Phosphor Thermography Data With the IHEAT Software Package , 36th AIAA Aerospace Sciences Meeting and Exhibit, Reno, Nevada, AIAA 98-0712, January 12-15, 1998, pp. 21, (3MB).

9 Wells, J.M., Jones, T.W., "Polarization techniques applied to enhance photogrammetric measurements of reflective surfaces," 46th AIAA/ASME/ASCE/AHS/ASC Structures, Structural Dynamics & Materials Conference, AIAA-2005-1887, Austin, Texas, April 2005.